

A Mathematical Model for Membrane Transport of Amino Acid and Na^+ in Vesicles

Anita K. Babcock*, Thomas Q. Garvey, III, and Mones Berman

Laboratory of Theoretical Biology, National Cancer Institute,
and Digestive Diseases Branch, National Institute of Arthritis, Metabolism,
and Digestive Diseases, National Institutes of Health, Bethesda, Maryland 20014

Received 19 January 1979; revised 13 April 1979

Summary. A model with a carrier having sites for both amino acid and Na^+ can account for AIB (α -aminoisobutyric acid) transport kinetics observed in membrane vesicles from SV3T3 (simian virus 40-transformed Balb/c3T3 cells) and 3T3 (the parent cell line). The main feature of this cotransport model is that Na^+ binding to carrier decreases the effective K_m for AIB transport. Na^+ transport kinetics observed in both vesicle systems can be described by passive (possibly facilitated) diffusion. The lag of Na^+ transport across the membrane compared to that for AIB, coupled to the Na^+ -dependent decrease in the K_m for AIB, accounts for the overshoot in intravesicular AIB observed for SV3T3 in the presence of an initial Na^+ gradient. Extra-vesicular Na^+ maintains a decrease in the K_m for AIB influx before intra-vesicular Na^+ has accumulated to balance it with a comparable decrease in the K_m for AIB efflux. 3T3 vesicles display little overshoot, and this finding can be explained mostly by a lower carrier affinity for Na^+ .

Much evidence suggests that a carrier mechanism capable of Na^+ cotransport mediates the concentrative uptake in mammalian cells of neutral amino acids, including the amino acid analog, AIB, α -aminoisobutyric acid [9, 21]. It has been shown on the basis of energetics [10] that the Na^+ electrochemical potential difference is theoretically capable of providing the driving force for this cotransport. Transport studies using membrane vesicles permit the establishment of defined concentration gradients for Na^+ , since vesicles contain a single compartment, in contrast to intact cells. Vesicles are also independent of any metabolic effects on transport and of metabolic energy sources for maintaining ion gradients.

The purpose of the present study is to develop a mathematical model that accounts for the observed uptake patterns for AIB and Na^+ across vesicle membranes with varied initial intra- and extravesicular Na^+

* Address for reprint requests: Building 10, Room 4B-56, National Institutes of Health, Bethesda, Maryland 20014.

concentrations [4]. With an initial Na^+ gradient and low initial intravesicular Na^+ concentration, an overshoot in intravesicular AIB can develop for vesicles from simian virus 40-transformed Balb/c3T3 cells, SV3T3 (see Fig. 2). Little overshoot is seen with the parent line (3T3). These kinetics are fully accounted for by a proposed model composed of a Na^+ -amino acid cotransport mechanism and a Na^+ effect on the affinity of the carrier for AIB.

Materials and Methods

The experimental methods used to generate the data analyzed here have been described in detail in the accompanying paper [7]. Briefly, vesicle preparations consisting of plasma membrane and endoplasmic reticulum were prepared from SV3T3 and 3T3 cells (mouse fibroblast cells). Vesicles from both sources appeared spherical and unilamellar under the electron microscope [7], and mean vesicle diameters for SV3T3 and 3T3, respectively, of 2700 and 2365 Å from normal distributions with 60% standard deviations were obtained using a quasi-elastic light scattering technique¹. Initial intravesicular Na^+ concentrations were established by equilibrating vesicles with a medium containing concentrations of NaCl varying from 0 to 100 mM. 0.1 mM ³H-labeled AIB with or without 100 mM NaCl was added to the vesicle medium, and the uptake kinetics of AIB and Na^+ were measured. Final values for uptake of AIB and Na^+ were assumed to reflect equilibration of intravesicular solvent water with extravesicular concentrations of these solutes, and equilibrium intravesicular concentrations were assumed to be the same as concentrations in the medium. With these assumptions, the solvent water for SV3T3 and 3T3 vesicles was estimated to be about 0.35 μl per mg of vesicle protein, and this value was used to calculate intravesicular concentrations required for comparison with extravesicular concentrations from the uptake values (moles/mg protein). Intravesicular solvent water volume could not be accurately measured to confirm the estimate [7].

If, however, it is assumed that most of the protein measured in the solutions of the vesicles is part of the relatively thin limiting membranes of spherical vesicles², solvent water for SV3T3 and 3T3 vesicles is calculated as $11.0 \pm 9.2 \mu\text{l}/\text{mg}$ protein and $9.5 \pm 8.0 \mu\text{l}/\text{mg}$ protein, respectively, using the mean vesicle diameters listed above. These last estimates of intravesicular solvent volume differ by a factor of 30 from the estimates made using equilibration data. The reasons for this difference are unclear. It is possible that only a small proportion of the total protein in the vesicle solutions is vesicle protein. This percentage, however, is uniform throughout the vesicle experiments, as indicated by the close correspondence of the equilibrium values for AIB uptake. Other possible explanations include heterogeneity in vesicle diameters measured as a 60% standard deviation that is far from negligible, membrane thickness greater than 80 Å, and distortion from a spherical vesicle shape during assays for uptake. The overshoot in intravesicular AIB could result from some physical change of a small fraction of the vesicles (10%) such that they pop

¹ G. Williams and D. Litster (*in preparation*).

² The expression used for calculating the intravesicular space was as follows:

$$(4/3) \pi (R - T)^3 / [(4/3) \pi R^3 - (4/3) \pi (R - T)^3] (f) (\rho_p),$$

where R is the outside radius, f is the fraction of membrane volume occupied by protein (0.33 ± 0.10 [18]), ρ_p is the density of membrane protein ($1.35 \pm 0.135 \text{ g/cm}^3$ [16]), and T is the membrane thickness ($80 \pm 8 \text{ Å}$).

and reseal after taking up Na⁺ ion if this fraction concentrates amino acid about 25-fold before they pop, but this possibility seems unlikely.

To fit all the data to a common model, it was observed that a constant background of about 20% of the final intravesicular concentration seems to be required. This may be due to medium trapped between vesicles after incomplete rinsing or to solute bound tightly to vesicles. This background concentration of AIB or Na⁺ was automatically computed for each curve during the fitting.

The modeling and data fitting were performed on a digital computer using the SAAM program [2]. SAAM iteratively adjusts initial estimates of parameter values, by computing partial derivatives, until a least squares fit is obtained.

Model Development

The model proposed here for membrane transport of AIB and Na⁺ consists of an intravesicular and an extravesicular compartment separated by a membrane in which AIB and Na⁺ must interact during transport. This interaction of AIB and Na⁺ is required to account for the observed overshoot in intravesicular AIB concentration during uptake in response to an initial Na⁺ gradient, as shown in Fig. 2*B*. A simpler model containing 2 compartments with first order transport kinetics for both AIB and Na⁺ cannot account for this overshoot.

A minimal model must predict the observed behavior of the system under all conditions of the experiments with the same set of parameter values. Several models were tested and discarded. In particular, a number of models using log functions of Na⁺ concentrations to describe an effect of the transmembrane Na⁺ electrochemical potential difference on the transport rate for amino acid could not predict uptake patterns for all initial Na⁺ concentrations with a single set of parameter values.

The amino acid-Na⁺ cotransport model proposed is shown in Fig. 1. X is the carrier in the membrane and A is the amino acid, AIB. The subscripts i and o represent the intra- and extravesicular regions, respectively. P is the carrier translocation rate constant, and the k_j are kinetic rate constants. In this model AIB is transported across the membrane by the carrier X either with or without Na⁺. It is assumed here that the carrier in all its forms translocates in both directions with the same rate constant, P . It is assumed that the membrane components are in a pseudo-equilibrium state, and consequently, $k_1/k_{-1} = k_4/k_{-4}$ and $k_2/k_{-2} = k_3/k_{-3}$ as a result of microscopic reversibility.

Equations (1) and (2) describe the kinetics of AIB and Na⁺ transport in the model. K_D^{AIB} and $K_D^{Na^+}$ are the respective dissociation constants from carrier for AIB and Na⁺, V_{max} is the maximum AIB transport rate possible, i.e., the product of the translocation rate constant, P ,

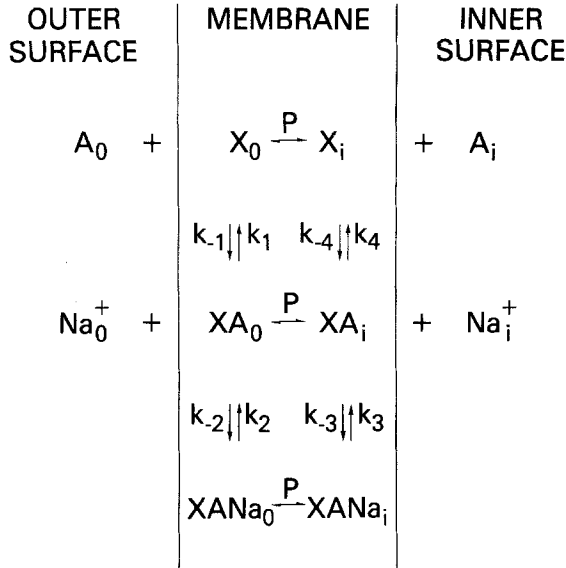


Fig. 1. Amino acid- Na^+ cotransport model. X =carrier, A =AIB, P =translocation rate, k_j =kinetic rate constants

and the carrier concentration, and L^{Na^+} is the rate constant for Na^+ transport.

$$\frac{d[A]_i}{dt} = \frac{V_{max}[A]_o}{K_D^{AIB} \frac{1}{1 + \frac{[Na^+]_o}{K_D^{Na^+}}} + [A]_o} - \frac{V_{max}[A]_i}{K_D^{AIB} \frac{1}{1 + \frac{[Na^+]_i}{K_D^{Na^+}}} + [A]_i} \tag{1}$$

$$\frac{d[Na^+]_i}{dt} = L^{Na^+} ([Na^+]_o - [Na^+]_i). \tag{2}$$

Equation (1) was derived by Curran *et al.* [4] for unidirectional transport of alanine across intestinal mucosa, assuming that translocation is rate limiting, and applied to steady state experiments. In essence, it says that transport of AIB is a Michaelis-Menten process and that the effective Michaelis-Menten constant for AIB is modulated by the Na^+ concentration:

$$K_m^{AIB} = K_D^{AIB} \frac{1}{1 + \frac{[Na^+]_o}{K_D^{Na^+}}}.$$

Equations (1) and (2) imply that all processes across the membrane are symmetric with respect to inside and outside.

Table 1. Model parameter values and their SD derived for the curves shown in Figs. 2 and 3

Parameter		Parameter									
$[\text{Na}^+]_b$ (mM)	$[\text{Na}^+]_i$ ($t=0$) (mM)	V_{\max} (mM min $^{-1}$)	K_D^{AIB} (mM)	$K_D^{\text{AIB}} \cdot K_D^{\text{Na}^+}$ (mM 2)	$K_D^{\text{Na}^+}$ (mM)	$V_{\max}/K_D^{\text{AIB}}$ (min $^{-1}$)	Background (AIB) (mM)	Fraction of vesicles transporting AIB and Na^+	L^{Na^+} (min $^{-1}$)		
SV3T3	0 ^a	0.41 ± 0.12	—	—	—	—	0.039 ± 0.002	0.047 ± 0.002	0.111 ± 0.008		
	100 ^b	0.34 ± 0.04	—	1.3 ± 0.5	—	—	0.000 ± 0.008	0.032 ± 0.002	(Na^+ background = 9 ± 2 mM)		
	101	0.62 ± 0.09	—	1.8 ± 0.6	—	—	0.10 ± 0.03	0.026 ± 0.001			
	102	0.56 ± 0.09	—	1.3 ± 0.4	—	—	0.01 ± 0.01	0.040 ± 0.004			
	104	0.53 ± 0.09	—	2.2 ± 0.7	—	—	0.08 ± 0.02	0.030 ± 0.004			
	110	0.52 ± 0.09	—	2.2 ± 0.8	—	—	0.14 ± 0.02	0.024 ± 0.004			
	120	0.45 ± 0.08	—	2.1 ± 0.7	—	—	0.02 ± 0.03	0.035 ± 0.006			
	150	0.27 ± 0.07	—	2.0 ± 0.7	—	—	0.00 ± 0.02	0.041 ± 0.006			
	200	0.51 ± 0.09	—	2.6 ± 0.7	—	—	0.00 ± 0.02	0.035 ± 0.006			
SV3T3 combined fit		0.38 ± 0.02	21 ± 8	—	0.12 ± 0.04	0.018 ± 0.007	0.029	0.034	0.111		
3T3 combined fit		0.14 ± 0.02	0.11 ± 0.05	—	8 ± 12	1.3 ± 0.6	0.029	0.034	0.111		

^a Parameters obtained by fitting data from four different experiments simultaneously to a common set of parameters.

^b Parameters obtained similarly from two sets of data.

Na^+ transport, Eq. (2), is adequately described by Fick's law, since fitting the data to the model showed that the component carried in association with AIB is only a small fraction of total Na^+ transport. This Na^+ transport may well occur by a facilitated, i.e., carrier-mediated, process.

Results

Na^+ kinetics were available only for the uptake study with vesicles initially depleted of Na^+ . Since the fractional standard deviation of the value of parameter L^{Na^+} derived from the fit to these data is small (see Table 1), this value of L^{Na^+} was used for analysis of all subsequent AIB uptake studies.

In the independent fitting of each individual study for SV3T3, V_{\max} and the product $K_D^{\text{AIB}} \cdot K_D^{\text{Na}^+}$ were the only parameters that could be

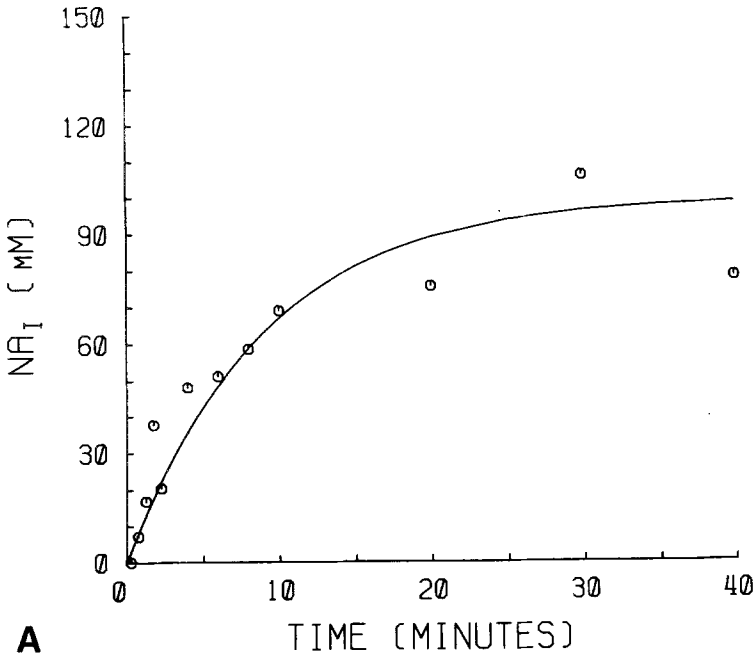
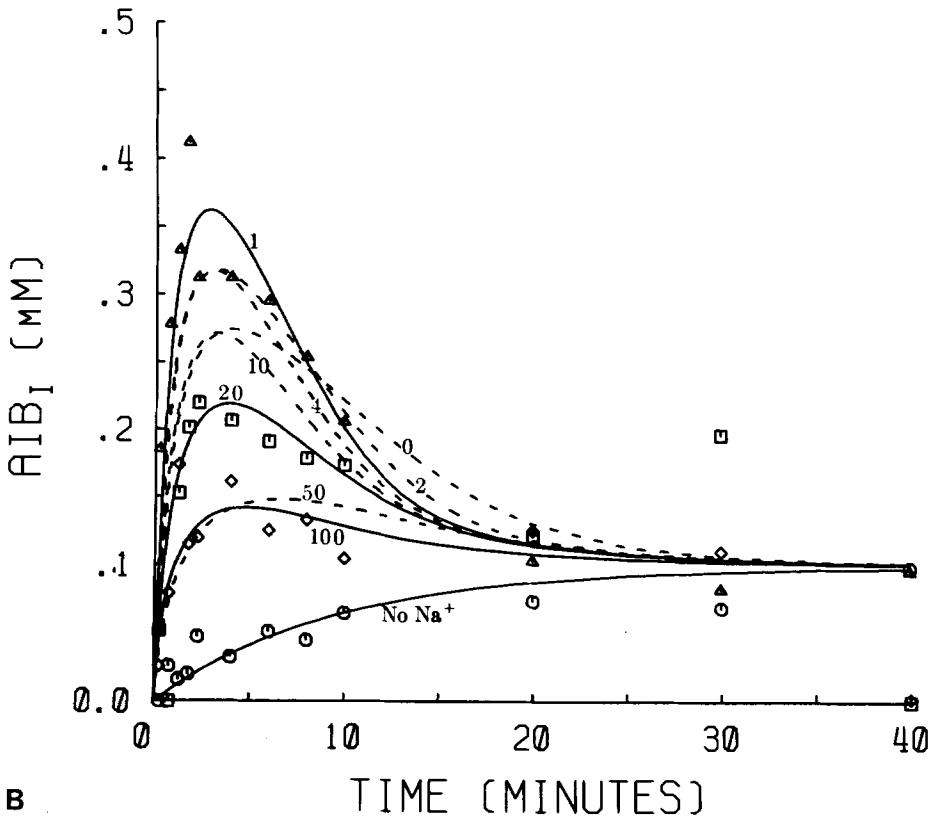


Fig. 2. Na^+ effect. (A): Kinetic behavior predicted from the model for Na^+ uptake into Na^+ -depleted vesicles in the presence of AIB uptake represented by line. Points in both A and B represent data obtained in previous studies [7]. (B): Na^+ -independent and Na^+ -dependent AIB uptake predicted from the model in fitting data for each Na^+ preloading level represented by solid and dashed lines. For $t=0$, $[\text{AIB}]_i=0.0$, $[\text{AIB}]_o=0.1 \text{ mM}$, $[\text{Na}^+]_o=100 \text{ mM} + [\text{Na}^+]_i$, and $[\text{Na}^+]_i$ is as shown. Four representative sets of data are shown, and dashed lines are shown without the corresponding data

determined with some confidence. When all the studies were fitted jointly, however, to a common set of parameters, some estimates of the individual parameters, K_D^{AIB} and $K_D^{Na^+}$, could also be obtained, although only within about 40% uncertainty. The results of these individual and joint studies are shown in Table 1.

Figure 2B shows the individual model-derived AIB uptake curves and representative data for SV3T3 in the presence of different initial intra- and extravesicular Na⁺ concentrations. Also shown (Fig. 2A) are the model-derived Na⁺ uptake curve and the corresponding data.

Kinetic patterns of AIB and Na⁺ transport in vesicles from non-transformed cells, 3T3, (which display little overshoot) can also be fitted by the model developed for SV3T3, as shown in Fig. 3. Two sets of data—one in the absence and one in the presence of an initial Na⁺ gradient—were fitted jointly to obtain a set of parameter values. Fractional standard deviations for parameter values were comparable with those for SV3T3 (Table 1). Kinetics of uptake of Na⁺ into 3T3-derived



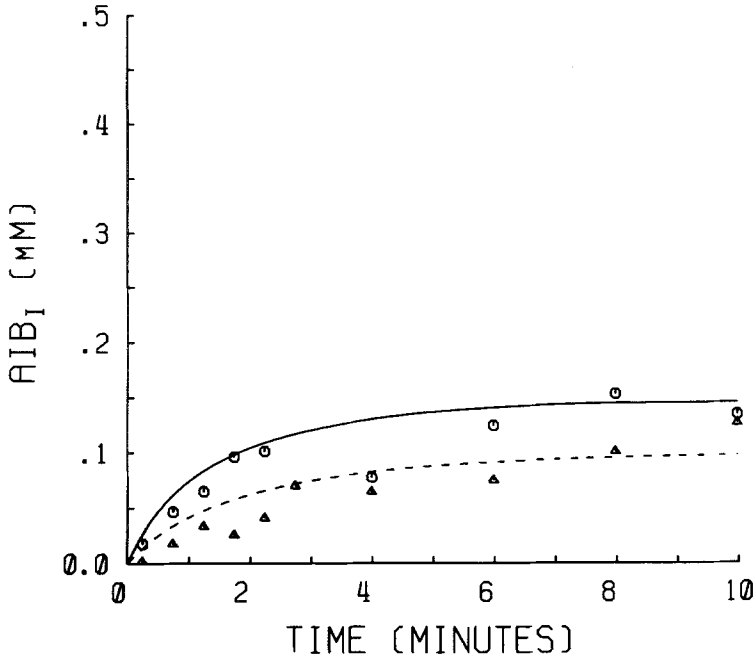


Fig. 3. Transformation effect. Na⁺-independent and Na⁺-dependent AIB uptake predicted from the model, with points representing previously published observed values in 3T3 [17]

vesicles were quantitatively similar to those for SV3T3-derived vesicles [7].

To test more rigorously the necessary and sufficient differences between the 3T3 and the SV3T3 cells, the two sets of data were fitted jointly, subject to certain hypotheses [1]. The same value of L^{Na^+} was used in both cases. First, we tested for the parameters that it was necessary to change. To establish this, each of the parameters in turn was held constant, and all other parameters allowed to vary in trying to refit the data. This led to the conclusion that $K_D^{\text{Na}^+}$ had to change in order to fit all the data simultaneously.

On the other hand, when the fitting was performed subject to the hypothesis that the only difference be a change in $K_D^{\text{Na}^+}$, it was found that this was not sufficient to account for the difference between the kinetic patterns in 3T3 and SV3T3 vesicles. It was found that, in addition to $K_D^{\text{Na}^+}$, a change in either V_{max} or K_D^{AIB} was necessary and sufficient to account for this difference. Furthermore, the changes in V_{max} or K_D^{AIB} were proportional, so that the best measure to account for the difference

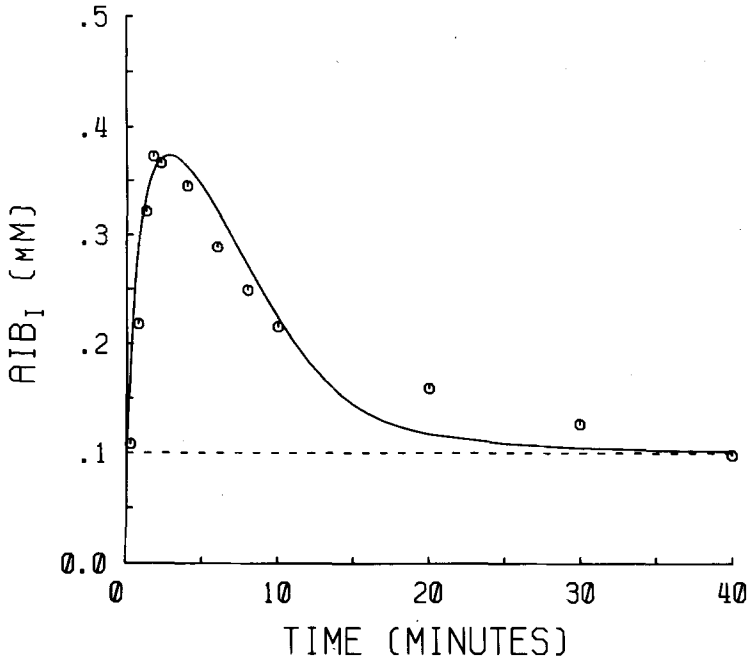


Fig. 4. Predictive ability of the model. Na^+ gradient-dependent AIB overshoot predicted for AIB preequilibration, with points that represent values observed in previous studies. For $t=0$, $[\text{AIB}]_i = [\text{AIB}]_o = 0.1 \text{ mM}$

is the ratio $V_{\max}/K_D^{\text{AIB}}$. The final values of the ratio $V_{\max}/K_D^{\text{AIB}}$ and $K_D^{\text{Na}^+}$ for 3T3 and SV3T3 are presented in Table 1.

For a different set of experimental conditions—vesicles preequilibrated with AIB—the reequilibration pattern for intravesicular AIB in response to the addition of Na^+ to the medium was generated by the model using mean parameters derived for vesicles from SV3T3. The simulated curve is plotted as the solid line along with a typical set of data in Fig. 4. The dashed line shows the equilibrium level of AIB present initially. The ability of the model to predict this reequilibration is apparent.

Discussion

The model proposed here, which consists of an amino acid carrier capable of Na^+ cotransport, together with a passive (possibly facilitated) diffusion component for Na^+ , can account for AIB and Na^+ transport

kinetics observed in membrane vesicles from SV3T3 and 3T3 cells. In particular, it accounts for a Na^+ gradient-dependent overshoot in intravesicular AIB in the former that is modulated by changes in the intra- and extravesicular Na^+ concentrations. In this model, the effective K_m for AIB transport is decreased by Na^+ binding to carrier. The magnitude of this effect depends on the dissociation constant for Na^+ , $K_D^{\text{Na}^+}$, (see Table 1). The Na^+ effect on the K_m for SV3T3 is about 40-fold greater than the effect for 3T3 cells. Slow equilibration of Na^+ across the membrane, as seen in Fig. 2, coupled to the Na^+ -dependent decrease in the K_m for AIB, accounts for the overshoot observed for SV3T3 during AIB uptake in the presence of an initial Na^+ gradient. Extra-vesicular Na^+ produces a sustained decrease in the K_m for, and acceleration of, AIB inflow before intravesicular Na^+ has built up to produce a comparable decrease in the K_m for AIB outflow.

The model generates re-equilibration patterns obtained from SV3T3 vesicles under experimental conditions independent of those used for its development, confirming its predictive ability. The model also describes AIB uptake patterns in 3T3 vesicles, which display little overshoot. The similarity of Na^+ uptake kinetics for 3T3 and SV3T3 rules out the possibility that relatively high Na^+ permeability in 3T3 vesicles might account for the decreased overshoot. This study identifies the differences in parameters responsible for these differences in transport kinetics, i.e., that $K_D^{\text{Na}^+}$ and $V_{\max}/K_D^{\text{AIB}}$ decrease with transformation. The Na^+ effect on the K_m for AIB influx for 3T3 is much smaller than that for SV3T3, and as a result there is much less difference between AIB inflow and outflow at early times.

The model introduces the idea that in transformed cells the carrier that mediates Na^+ -dependent transport of a nonelectrolyte has a higher affinity for Na^+ than the corresponding carrier in untransformed cells. This suggestion raises the question whether the increase in carrier affinity for Na^+ is the property of any rapidly dividing cell or is specific to virus transformation. The model can be used to test the first possibility by the analysis of a comprehensive set of transport studies of the type analyzed in the present paper, using both embryonic and mature cell lines.

Alternative good models that account for amino acid and Na^+ transport kinetics for each Na^+ concentration with the same parameter values are difficult to identify, as previously mentioned.

Although a direct effect of membrane potential in the model is unnecessary to fit the data, the Na^+ dependent decrease in the effective K_m

for AIB transport may result from Na⁺-induced, energy-dependent conformational changes in the amino acid binding site, such as those known to occur in many allosteric systems [3]. For intact cells the available evidence suggests [19] that the ternary complex between carrier, amino acid, and Na⁺ can translocate in a charged form. Therefore, the presence of a membrane potential difference might influence the rate of this translocation.

The model predicts that for typical Na⁺ concentrations in intact cells ($[Na^+]_o = 150 \text{ mM}$, $[Na^+]_i = 15 \text{ mM}$ [22]), assuming uniform distribution of Na⁺ in the cell, the distribution ratio of intra- to extracellular AIB would be about 10 for transformed cells and about 7 for non-transformed cells. Experiments conducted with confluent intact cells from lines similar to those we have used [6] have also produced evidence that transformed cells concentrate AIB to a greater extent than the untransformed parent line, with distribution ratios of 22 and 12, respectively. Problems with cell volume, intracellular compartmentation, membrane potentials, and coupled metabolic reactions are not taken into account in this comparison and may account for the differences. Since the rate constant, L^{Na^+} , for Na⁺ transport in intact cells is probably a composite of free diffusion and membrane potential-dependent movement, Eq. (2) for Na⁺ transport in vesicles would have to be modified to predict intracellular Na⁺ concentrations in intact cells. Nonetheless, these findings are consistent with the suggestions of others [11] that the greater concentrations of amino acid in transformed cells may control tumor growth.

It has been suggested by some that a Na⁺-dependent AIB exchange diffusion is important in Na⁺-dependent AIB transport in Ehrlich ascites cells [13]. These trans effects were not necessary to fit the data, although loading experiments might resolve them.

Inclusion of a diffusion component for AIB at the relatively low extraventricular concentration of 0.1 mM used in all experiments from which the model was developed was also found unnecessary, in agreement with data on AIB uptake from low extraventricular AIB concentration experiments in the placental microvillus vesicle system [20].

Na⁺-dependence of V_{max} has been observed in initial flux experiments using Ehrlich ascites cells [13]. We, however, did not observe a large change in V_{max} over the range of Na⁺ concentrations studied. The explanation for this difference may lie in the different experimental conditions. In the experiments with Ehrlich ascites cells, the greatest changes in V_{max} appeared in the range of Na⁺ concentrations from 0–30 mM, while

at higher Na^+ concentrations the change in V_{\max} observed [13] was about 15–20%, which is within the fractional standard deviation obtained for the parameter V_{\max} from the present analysis (see Table 1).

For initial flux experiments the model can predict the effective K_m for AIB for any Na^+ concentration. Comparison of these calculated values can be made directly with literature values, although the unlikelihood of measuring true initial velocities in uptake studies makes it difficult to obtain reliable K_m values. The model predicts the effective K_m for the Na^+ -dependent part of the alanine transport in pancreas-derived vesicles [23]. However, the model-derived values for the effective K_m for AIB uptake by Ehrlich ascites tumor cells [13] and SV3T3 vesicles and cells [8, 12, 14] are only about 1% of the literature values. A dual transport system may well be responsible for this difference. Renal brush border membrane vesicles exhibit two K_m 's, $K_{m1}=0.067$ mM and $K_{m2}=5.26$ mM for proline transport and $K_{m1}=0.22$ mM and $K_{m2}=4.0$ mM for glycine transport [15,5]. The low K_m for transport of these neutral amino acids is consistent with the model-derived K_m values in our experiments carried out with low extra-vesicular AIB concentrations of 0.1 mM. The low K_m values are probably also consistent with physiological concentrations for amino acids [24] and may be most relevant in physiological regulation of transport.

References

1. Berman, M. 1963. A postulate to aid in model building. *J. Theor. Biol.* **4**:229
2. Berman, M., Weiss, M.F. 1967. SAAM Manual. (U.S. Public Health Service Publication No. 1703) U.S. Government Printing Office, Washington
3. Blumenthal, R., Changeux, J.-P., Lefever, R. 1970. Membrane excitability and dissipative instabilities. *J. Membrane Biol.* **2**:351
4. Curran, P.F., Schultz, S.G., Chez, R.A., Fuisz, R.E. 1967. Kinetic relations of Na-amino acid interaction at mucosal border of intestine. *J. Gen. Physiol.* **50**:1261
5. Fass, S.J., Hammerman, M.R., Sacktor, B. 1977. Transport of amino acids in renal brush border membrane vesicles. Uptake of the neutral amino acid L-alanine. *J. Biol. Chem.* **252**:583
6. Foster, D.O., Pardee, A.B. 1969. Transport of amino acids by confluent and nonconfluent 3T3 and polyoma virus-transformed 3T3 cells growing on glass cover slips. *J. Biol. Chem.* **244**:2675
7. Garvey, T.Q., Babcock, A. 1979. Amino acid and $^{22}\text{Na}^+$ uptake in membrane vesicles from confluent simian virus 40 transformed Balb/c3T3 and Balb/c3T3. *J. Membrane Biol.* **49**:139
8. Hamilton, R., Nilsen-Hamilton, M. 1976. Sodium-stimulated alpha-aminoisobutyric acid transport by membrane vesicles from simian virus-transformed mouse cells. *Proc. Nat. Acad. Sci. USA* **73**:1907

9. Heinz, E., editor. 1972. Na⁺-Linked Transport of Organic Solutes. Springer-Verlag, New York
10. Heinz, E., Geck, P. 1974. The efficiency of energetic coupling between Na⁺ flow and amino acid transport in Ehrlich cells—a revised assessment. *Biochim. Biophys. Acta* **339**:426
11. Holley, R.W. 1972. Increased uptake of amino acids and 2-deoxy-D-glucose by virus-transformed cells in culture. *Proc. Nat. Acad. Sci. USA* **69**:2840
12. Isselbacher, K.J. 1972. Increased uptake of amino acids and 2-deoxy-D-glucose by virus-transformed cells in culture. *Proc. Nat. Acad. Sci. USA* **69**:585
13. Jacquez, J.A. 1973. Sodium dependence of maximum flux, J_M , and K_M of amino acid transport in Ehrlich ascites cells. *Biochim. Biophys. Acta* **318**:411
14. Lever, J.E. 1976. Regulation of amino acid and glucose transport activity expressed in isolated membranes from untransformed and SV 40-transformed mouse fibroblasts. *J. Cell. Physiol.* **89**:779
15. McNamara, P.D., Ozegovic, B., Pepe, L.M., Segal, S. 1976. Proline and glycine uptake by renal brushborder membrane vesicles. *Proc. Nat. Acad. Sci. USA* **69**:4521
16. Nelson, G.J., editor. 1972. Blood Lipids and Lipoproteins. p. 475. Wiley-Interscience, New York
17. Parnes, J.R., Garvey, T.Q., Isselbacher, K.J. 1976. Amino acid transport by membrane vesicles of virally transformed and nontransformed cells: Effects of sodium gradient and cell density. *J. Cell. Physiol.* **89**:789
18. Quinn, P.J. 1976. The Molecular Biology of Cell Membranes, p. 82, University Park Press, Baltimore
19. Reid, M., Gibb, L.E., Eddy, A.A. 1974. Ionophore-mediated coupling between ion fluxes and amino acid absorption in mouse ascites-tumour. *Biochem. J.* **140**:383
20. Ruzycski, S.M., Kelley, L.K., Smith, C.H. 1978. Placental amino acid uptake. IV. Transport by microvillous membrane vesicles. *Am. J. Physiol.* **234**:C27
21. Schultz, S.G., Curran, P.F. 1970. Coupled transport of sodium and organic solutes. *Physiol. Rev.* **50**:637
22. Snell, F.M., Shulman, S., Spencer, R.P., Moos, C. 1965. Biophysical Principles of Structure and Function, p. 317. Addison Wesley, Reading
23. Tyrakowski, T., Milutinovic, S., Schultz, I. 1978. Studies on isolated subcellular components of cat pancreas. III. Alanine-sodium cotransport in isolated plasma membrane vesicles. *J. Membrane Biol.* **38**:333
24. Vaughan, V.C., McKay, R.J., editors. 1975. Nelson Textbook of Pediatrics, p. 1783. W.B. Saunders, Philadelphia